Second phase strengthening mechanism of 2219 aluminum alloy

Haiyan Lin[1, a], Xianchang Mao[1, b], Tugan Lin [1, c], and Jun Wei [1, d]

[1]School of Automotive Engineering, Guangxi Transport Vocational and Technical college, Nanning, 530023, China.

[a] 1583491244@qq.com, [b] mxchlhy@163.com, [c] 940567356 @qq.com, [d] nnweijunhao@126.com

Abstract. Second phase particles have a decisive role in strengthening 2219 aluminum alloy, so it is important to study its strengthening mechanism. The different characteristics of the second phase particles of 2219 aluminum alloy were summarized, and the strengthening mechanism of deformable second phase particles (strain strengthening, chemical strengthening, order strengthening, modulus strengthening) and non-deformable second phase particles was analyzed. The strengthening mechanism model was established, the main application of the two particles was explained, and the guiding significance of the second phase particles on the coarse residual crystal phase breaking and the grain microstructure refinement of aluminum alloy was pointed out.

Keywords: 2219 aluminium alloy; strengthening mechanism; deformable particles; non-deformable particles.

1. Introduction

Due to its high specific strength, good mechanical properties at low and high temperatures, high fracture toughness, and good stress corrosion resistance, 2219 aluminum alloy has been widely used in aerospace, automobile manufacturing, machinery manufacturing, construction industry, shipbuilding and other fields to manufacture high-strength, high-hardness parts and structural parts [1-3]. 2219 aluminum alloy belongs to the second phase particle strengthening deformation aluminum alloy, in the "high temperature solid solution and aging" heat treatment process, with the strengthening effect of the second phase particles, 2219 aluminum alloy mechanical properties have been greatly improved [4-5]. Therefore, the second phase particle strengthening mechanism of aluminum alloy has always been a research hotspot in the industry, which has also been paid attention to by scholars [6-8], and many valuable research results have been obtained [9-11]. In this work, different types of second phase particles are summarized and different strengthening mechanisms of second phase particles are analyzed, so as to provide more comprehensive theoretical knowledge of second phase strengthening for the industry, and provide reference for expanding the application of 2219 aluminum alloy and improving product quality.

2. Deformable particles strengthening

The deformable second phase particles in 2219 aluminum alloy mainly include θ' phase (chemical formula Al2Cu) and θ "phase (chemical formula Al3Cu) under underaging and peak aging. The θ "phase appears as a disc-shaped in three dimensions, with a thickness of about 0.8~2 nm and a diameter of about 14 nm. The θ' phase is also disc-shaped in three dimensions, with a thickness of about 7~10 nm and a diameter of about 100 nm. The two strengthening phases can coexist in 2219 aluminum alloy, as shown in Fig. 1.

2.1 Coherent strain strengthening

The θ' and θ' phases are coherent or semi-coherent with the aluminum matrix, and they produce coherent strain fields with the matrix, as shown in Fig. 2. During the plastic deformation of 2219 aluminum alloy, the dislocation cuts through the θ' and θ' phases.At this time, θ' and θ' phases are equivalent to mismatched spheres, and strong elastic interaction occurs between the coherent stress-strain field and the dislocation. Cu atom enrichment on the Al (100) plane causes tensile stress on the matrix lattice, that is, the coherent strain strengthening of the precipitated phase is formed.

For the elastic interaction between the mismatch ball and the dislocation, the increment of critical shear stress when the dislocation cuts through the precipitated phase is expressed by the following formula.

$$\tau_c = \beta \cdot G \cdot \varepsilon^{2/3} \cdot f^{\frac{1}{2}} \cdot \left(\frac{r}{b}\right)^{1/2} \tag{1}$$

Where, f is the volume fraction of precipitated phase particles; ε is the coherent strain; r is the radius of precipitated phase particles; b is the Burgess vector; G is the shear modulus of aluminum matrix. β is a constant, 3 for edge dislocation and 1 for screw dislocation. It can be seen from formula (1) that the larger the coherent strain value and the volume fraction of the precipitated phase, the better the strengthening effect of the precipitation relative to the alloy. The larger the amount of precipitated phase and the larger the volume fraction, the larger the total coherent strain variable in the alloy. Therefore, increasing the volume fraction of the precipitated phase in the alloy is the most direct way to improve the strengthening effect of the alloy.

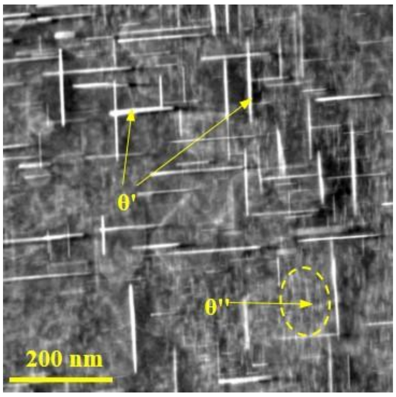

Fig. 1 TEM morphology of deformable second phase particles of 2219 aluminum alloy

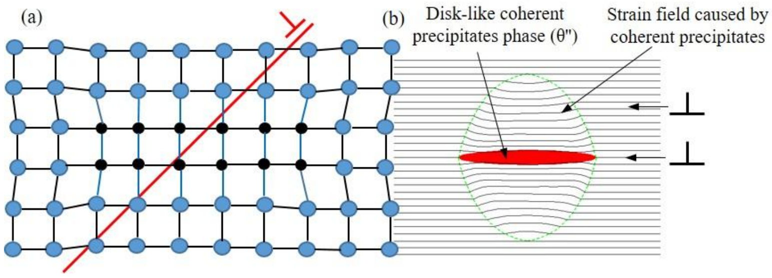

Fig. 2 Strain strengthening model of Al-Cu alloy: (a) coherent particles; (b) coherent strain field

2.2 Chemical strengthening

When the dislocation cuts through the θ' and θ''phases, the disk-like second phase particles (θ and θ phases) are cut open and a displacement appear on the cutting surface to form a new interface (Fig. 3). The new interface leads to the increase of the contact area between the second phase and the aluminum matrix, which leads to the increase of energy. Furthermore, the structure of the second phase is different from that of the matrix, when the dislocation sweeps through the fine precipitated phase, the local atomic dislocation inevitably cause the resistance of dislocation migration to increase, and the alloy can be strengthened. This strengthening is called chemical strengthening.

The increment of critical shear stress caused by chemical strengthening can be represented by the following model.

$$\tau_c = \frac{2\sqrt{6}}{\pi} \cdot \frac{f \cdot \gamma_s}{r} \tag{2}$$

Where, f is the volume fraction of precipitated phase; r is the radius of precipitated phase particles; γs is the interface energy. It can be seen from the formula that the larger the volume fraction of precipitated phase, the smaller the particle radius, and the larger the critical shear stress increment.

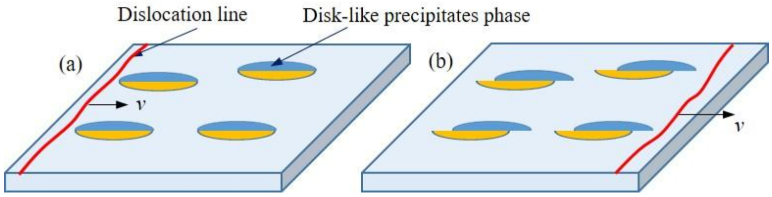

Fig. 3 Chemical strengthening model of 2219 aluminum alloy when dislocation cut precipitated particles: (a) before cutting; (b) after cutting

2.3 Ordered strengthening

The chemical formula of θ' and θ' phase are Al2Cu and Al3Cu, respectively, which are intermetallic compounds, and have an ordered lattice structure in the alloy. The θ' and θ' phases maintain a semi-coherent and coherent relationship with the matrix. When the dislocation cuts through the ordered strengthened phase particles, Antiphase boundary (APB) will be generated, which increases the energy of the alloy system and improves the strengthening effect, as shown in Fig. 4.

The increment of critical shear stress caused by ordered strengthening can be expressed by the following formula.

$$\tau_c = \frac{\gamma}{2b}[\left(\frac{4\gamma \cdot r \cdot f}{\pi T}\right)^{\frac{1}{2}} - f] \tag{3}$$

Where, γ is the antiphase domain boundary energy; b is the Bergdahl vector of dislocation; r is the radius of precipitated phase particles; f is the volume fraction of precipitated phase; T is the line tension of the dislocation line. It can be seen that increasing the size of precipitated particles is conducive to increasing the critical shear stress.

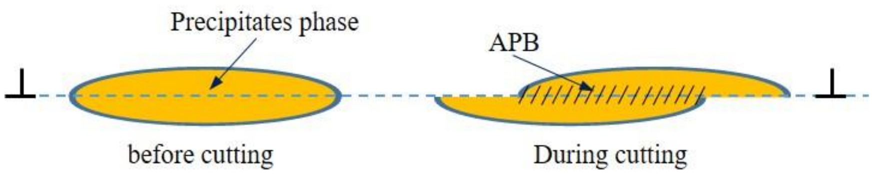

Fig. 4 Ordered strengthening model of 2219 aluminum alloy when dislocation cut precipitated particles

2.4 Modulus strengthening

The elastic modulus of the aluminum matrix of 2219 aluminum alloy is different from that of the θ' precipitated phase particle, as shown in Table 1. In the deformation process, when the dislocation line cuts through the particle, its own energy changes, resulting in alloy strengthening, that is, modulus strengthening.

In general, when the dislocation line enters from the aluminum matrix (soft phase) into the precipitated phase particles (hard phase), the energy increases, and the strength of the alloy is increased. Then, when the dislocation line moves out of the precipitated phase particles and enters the aluminum matrix, the capacity and strengthening effect decrease. The critical stress increment model caused by modulus strengthening is as follows.

$$\tau_c = \frac{0.8Gb}{L}\left(1 - \frac{E_1^2}{E_2^2}\right) \tag{4}$$

Where, E1 is the elastic modulus of the soft phase; E2 is the elastic modulus of the hard phase. G is the shear modulus of the base material. L is the average distance between the particles. It can be seen that the larger the difference of elastic modulus ΔE (E2- E1) between the soft phase and the hard phase and the smaller the distance L between precipitated particles, the larger the critical stress increment and the more significant the strengthening effect of the alloy.

Base on the above strengthening mechanisms, it can be seen that increasing the number of precipitated phase and reducing the spacing of precipitated phase are the main ways to improve the strengthening effect of 2219 aluminum alloy. The strengthening of the alloy may be a combination of the above strengthening mechanisms, or it may be one of them. Generally, when the coherent strain variable is large enough, that is, when the amount of precipitated phase in 2219 aluminum alloy is large enough, the coherent strain strengthening plays a major role in strengthening.

Table 1 Elastic modulus and hardness of aluminum matrix and Al2Cu particles

Index	Materials	Temperature /°C				
		25	200	240	280	320
Elastic modulus /GPa	α-Al	108.14	27.31	23.22	18.48	15.41
	Al_2Cu	181.21	61.01	55.24	48.34	44.12
Hardness /GPa	α-Al	1.74	0.67	0.58	0.49	0.41
	Al_2Cu	9.56	5.96	5.34	4.74	4.21

3. Non-deformable particle strengthening

The non-deformable particles in 2219 aluminum alloy mainly include residual crystalline phase, the secondary phase particles (θ phase, Al2Cu) formed by over-aging, and the T phase (Al20Cu2Mn3) which is difficult to dissolve, as shown in Fig. 5.

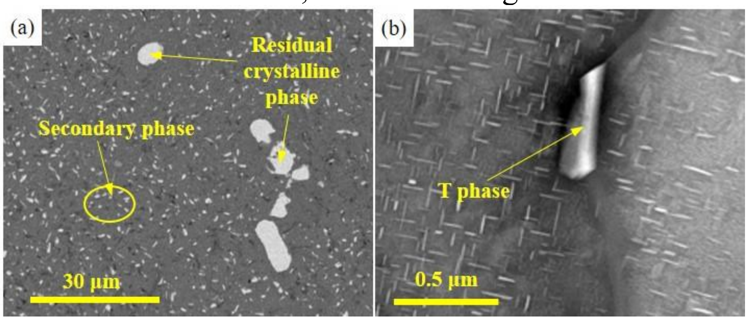

Fig. 5 Non-deformable second phase particles of 2219 aluminum alloy: (a) θ phase; (b) T phase

The size of the above three particles is large compared to the strengthened phase (θ' or θ ''), and the dislocation cannot be cut but bypassed during migration, as shown in Fig. 6. When the dislocation meets the dispersive non-deformable particles in the process of movement, its migration rate is decreased, the system energy increases, and the alloy is strengthened. This strengthening is called dispersion strengthening. The dispersion strengthening of aluminum alloy can be represented by Orowan model.

$$\sigma_c = \frac{Gb}{L} \tag{5}$$

Where σc is the critical shear stress at which the dislocation bypasses the second phase; G is the shear modulus of the matrix. L is the distance between the hard particles.

As can be seen from formula (5), the smaller the distance between hard particles, the more difficult it is for dislocations to bypass particles, the larger the energy increment of the system, the greater the critical shear stress of dislocations bypassing the second phase, and the more significant the alloy strengthening effect. During the plastic deformation of 2219 aluminum alloy, the dislocation forms a ring of dislocation around the particle when it bypasses the non-deformable particles. The dislocation rings can increase the hardness and strength of the matrix material around the particles.

However, the Orowan model does not take into account the size of the hard particle and the phase boundary repulsion of the dislocation line, as shown in Fig. 7a. The actual particle size can not be ignored, the residual crystal phase size of 5~30 μm, T-phase and secondary phase particle size of 0.2~2 μm. When a dislocation wraps around a particle, there is a certain distance between the dislocation line and the particle, as shown in Fig. 7b. The actual effective particle spacing can be obtained by considering the repulsive force of the phase boundary against the dislocation line and the particle size.

$$Le=L-d-2x \tag{6}$$

In general, x=0.1d, then Le=L-1.2d. Therefore, the formula (5) can be transformed into the follow formula.

$$\sigma_c = \frac{Gb}{L-1.2d} \tag{7}$$

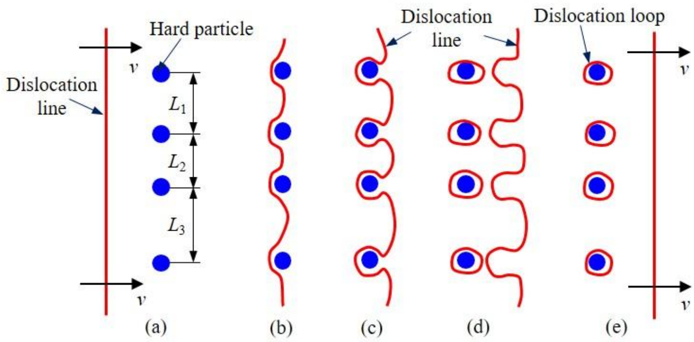

Fig. 6 Principle of dislocation ring formation around hard particles

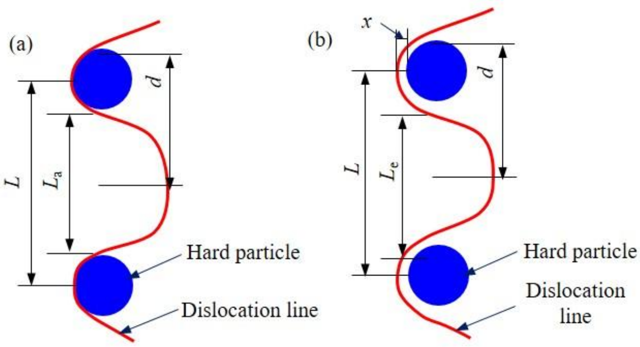

Fig. 7 Principle of effective distance between hard particles: (a) the effect of interface repulsion is not considered; (b) the effects of interface repulsion and particle size are considered

Further analysis shows that when the dislocation bypasses the obstacle particles, the abnormal dislocation of the curved neck can attract and destroy each other to achieve strengthening, as shown in Fig. 8. Therefore, the size of the neck R is the key to affecting the strengthening effect of the alloy. According to the model in Fig. 8, the critical condition under which the dislocation can bypass the particle can be calculated by the following formula.

$$F = 2T_1 \cdot \cos\frac{\varphi}{2} = \sigma_c \cdot b \cdot L \tag{8}$$

Formula (8) can be converted to

$$\sigma_c = \frac{2T_1}{b \cdot L} \cdot \cos\frac{\varphi}{2} \tag{9}$$

In addition, the force T (Fig. 8) can be represented by the following formula.

$$T_1 = \frac{Gb^2}{4\pi k_1} \cdot \ln\frac{R}{r_0} \tag{10}$$

Substituting formula (10) into formula (9) yields the following formula.

$$\sigma_c = \frac{Gb}{2\pi k_1 \cdot L} \cdot \ln\frac{R}{r_0} \cdot \cos\frac{\varphi}{2} \tag{11}$$

Where, R is the distance of the dislocation around the starting neck, usually R=3d; r0 is the central dimension of the dislocation, usually r0=b; k1 is the coefficient related to the properties of the dislocation, usually k1=1. Therefore, formula (11) can be transformed into the following formula.

$$\sigma_c = \frac{Gb}{2\pi \cdot L} \cdot \ln\frac{3d}{b} \cdot \cos\frac{\varphi}{2} \tag{12}$$

However, the deformation disharmony between the hard particles and the matrix is not taken into account in the above model. Since the critical shear stress is only related to the initial plastic deformation, the incompatibility of the two phases in the elastic deformation stage should be considered. The incompatibility model of elastic deformation between hard particles and matrix materials is shown in Fig. 9. It can be seen from Fig. 9b that under the action of external force, assuming that no particles exist in the matrix and only a hole is left, the hole would be deformed. However, in the presence of hard particles, assuming that the particles are deformed, the holes cannot be deformed freely. In order to maintain the continuity of the phase boundary, the matrix generates additional deformation force, making the holes return to a spherical shape (Fig. 9c). Therefore, the presence of hard particles generates an additional shear stress opposite to the external stress near the particles, as shown in Fig. 9d.

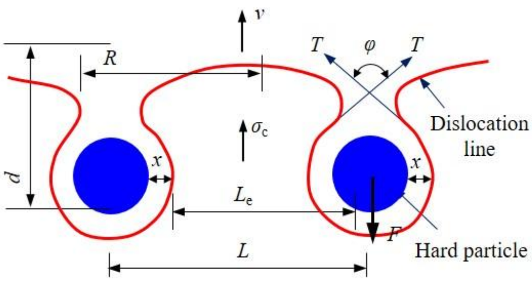

Fig. 8 Model of the bending threshold of a dislocation around hard particle

Considering the deformation disharmony between the hard particle and the matrix, the equivalent shear stress σe can be expressed by the following formula.

$$\sigma_o - \sigma_i = \frac{Gb}{2\pi \cdot L} \cdot \ln\frac{3d}{b} \cdot \cos\frac{\varphi}{2} \tag{13}$$

After adjusting formula (13), the following relatively more reasonable strengthening model can be obtained.

$$\sigma_o = \sigma_i + \frac{Gb}{2\pi \cdot L} \cdot \ln\frac{3d}{b} \cdot \cos\frac{\varphi}{2} \tag{14}$$

Where, σo is the yield strength of the alloy; σi is the additional shear stress opposite to the external stress σo, which is mainly affected by the size of the hard particle and is proportional to the reciprocal of the particle radius r to the third power.

$$\sigma_i \propto \frac{1}{r^3} \tag{15}$$

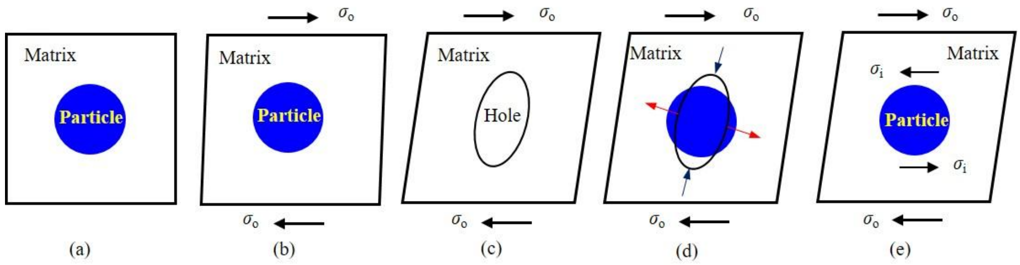

Fig. 9 Deformation disharmony model between hard particles and matrix: (a) Before deformation; (b) Elastic shear occurs in the matrix under external shear stress; (c) Assuming that there are only holes, the holes undergo shear under the action of external shear forces;(d) there are particles, the particles prevent the hole from deforming and cause additional deformation of the matrix;(e) Reverse additional shear stress occurs in the matrix around the particle

4. Summary

(1) The second phase particle strengthening of 2219 aluminum alloy can be divided into deformable particles strengthening of (soft particles, such as θ' phase and θ' phase) and non-deformable particles strengthening (hard points, such as θ phase and coarse residual crystal phase), the former is cut through by dislocations, the latter is bypassed by dislocations.

(2) Increasing the number of deformable strengthening particles and reducing the spacing of deformable strengthening particles is the key to improve the strengthening effect of 2219 aluminum alloy. The strengthening of the alloy may be the comprehensive effect of several strengthening mechanisms. When the strain is large enough, the common strain strengthening is the main strengthening mechanism of 2219 aluminum alloy.

(3) Deformable particle strengthening is mainly used to improve the mechanical properties of 2219 aluminum alloy structural parts during service. Non-deformable particle strengthening mainly occurs in the plastic deformation process of 2219 aluminum alloy, which increases the strength of aluminum matrix, improves the crushing ability of aluminum matrix to coarse residual crystalline phase, and increases the static recrystallization nucleation rate of the alloy.

5. Acknowledgement

The corresponding author is Xianchang Mao. This work was financially supported by Guangxi Natural Science Foundation (Grant No. 2020GXNSFAA159156), Guangxi Education Department research project Foundation (Grant No. 2023KY1152).

References

[1] CHEN Rui, WANG Yu, XIE Dan, et al. Multidirectional upsetting and stretching process of heavy 2219 aluminum alloy ingot [J]. Journal of Plasticity Engineering, 2022, 3: 25-33.

[2] Babu S, Panigrahi S, JanakiRam G, et al. Cold metal transfer welding of aluminium alloy AA 2219 to austenitic stainless steel AISI 321 [J]. Journal of Materials Processing Technology, 2019, 266: 155-164.

[3] Tian S, Chen W, Chen S, et al. The effect of cryogenic applications on tensile strength of aluminum 2219-T87 T-joint welded by dual laser-beam bilateral synchronous welding [J]. Journal of Manufacturing Processes, 2020, 56: 777-785.

[4] Fei Dong, Youping Yi, Shiquan Huang, et al. Refinement of second-phase particles and grain structures of 2219 Al – Cu alloy forgings using an improved thermomechanical treatment process[J]. Materials Characterization, 2021, 173:110927.

[5] Guo W F, Yi Y P, Huang S Q, et al. Effects of deformation temperature on the evolution of second-phase and mechanical properties of large 2219 Al-Cu alloy rings [J]. Materials Characterization, 2020, 160: 110094.

[6] Zhu H, Huang L, Li J, et al. Strengthening mechanism in laser-welded 2219 aluminium alloy under the cooperative effects of aging treatment and pulsed electromagnetic loadings [J]. Materials Science and Engineering: A, 2018, 714: 124-139.

[7] Takeda M, Maeda Y, Yoshida A, et al. Discontinuity of G.P.(I) zone and θ′-phase in an Al-Cu alloy [J]. Scripta Materialia, 1999, 41(6): 643-649.

[8] Da S, Xin Z, Ling Y, et al. Evolution of θ′ precipitate in aluminum alloy 2519A impacted by split Hopkinson bar [J]. Materials Science and Engineering: A, 2015, 620: 241-245.

[9] Hailin He, Youping Yi, Shiquan Huang, Yuxun Zhang. Effects of deformation temperature on second-phase particles and mechanical properties of 2219 Al-Cu alloy [J]. Materials Science & Engineering A, 2018, 712: 414–423.

[10] Xu D F, Chen S Y, Yu F, et al. Composition segregation behavior of 2219 aluminum alloy ingot with big size and effect of multi-axial forging and solution-aging treatment on microstructure and mechanical properties of ingot [J]. The Chinese Journal of Nonferrous Metals, 2017, 27(12): 2451-2459.

[11] Xianchang Mao, Youping Yi , Shiquan Huang, et al. Effects of warm saddle forging deformation on the reduction of second-phase particles and control of the three-dimensional mechanical properties of 2219 aluminum alloy rings[J]. Materials Science & Engineering A, 2021, 804: 140737.